Lab on a Chip

Cite this: *Lab Chip*, 2012, **12**, 1508

www.rsc.org/loc

PAPER

Efficient on-chip isolation of HIV subtypes

ShuQi Wang,†[a] Matin Esfahani,†[a] Umut A. Gurkan,[a] Fatih Inci,[a] Daniel R. Kuritzkes[b] and Utkan Demirci*[ac]

Received 1st August 2011, Accepted 6th January 2012
DOI: 10.1039/c2lc20706k

HIV has caused a global pandemic over the last three decades. There is an unmet need to develop point-of-care (POC) viral load diagnostics to initiate and monitor antiretroviral treatment in resource-constrained settings. Particularly, geographical distribution of HIV subtypes poses significant challenges for POC immunoassays. Here, we demonstrated a microfluidic device that can effectively capture various subtypes of HIV particles through anti-gp120 antibodies, which were immobilized on the microchannel surface. We first optimized an antibody immobilization process using fluorescent antibodies, quantum dot staining and AFM studies. The results showed that anti-gp120 antibodies were immobilized on the microchannel surface with an elevated antibody density and uniform antibody orientation using a Protein G-based surface chemistry. Further, RT-qPCR analysis showed that HIV particles of subtypes A, B and C were captured repeatably with high efficiencies of 77.2 ± 13.2%, 82.1 ± 18.8, and 80.9 ± 14.0% from culture supernatant, and 73.2 ± 13.6, 74.4 ± 14.6 and 78.3 ± 13.3% from spiked whole blood at a viral load of 1000 copies per mL, respectively. HIV particles of subtypes A, B and C were captured with high efficiencies of 81.8 ± 9.4%, 72.5 ± 18.7, and 87.8 ± 3.2% from culture supernatant, and 74.6 ± 12.9, 75.5 ± 6.7 and 69.7 ± 9.5% from spiked whole blood at a viral load of 10 000 copies per mL, respectively. The presented immuno-sensing device enables the development of POC on-chip technologies to monitor viral load and guide antiretroviral treatment (ART) in resource-constrained settings.

Introduction

33.3 million people are living with HIV-1 worldwide, with Sub-Saharan Africa accounting for 67% of the infected population.[1] To curb this pandemic, the World Health Organization (WHO) is rapidly expanding the number of AIDS patients receiving antiretroviral therapy (ART) in resource-constrained settings. These efforts, however, are significantly restricted by the prohibitive cost to implement ART monitoring tools, *i.e.*, CD4 cell counts by flow cytometry, and HIV viral load monitoring by reverse transcription-quantitative polymerase chain reaction (RT-qPCR). To address this challenge, various portable CD4 cell counting methods have been developed, including electrical sensing,[2] microfluidic lensless imaging,[3–6] fluorescence staining,[7,8] microscopy counting[9,10] and flow cytometry.[11] Although CD4 cell count in combination with WHO disease staging is widely used to monitor patients, studies have shown that CD4 monitoring cannot detect early treatment failure that may result in poor clinical outcomes such as development of drug resistance and early death.[12–14] Existing viral load tests are not routinely performed at the point-of-care (POC), since they require expensive instruments and reagents, skilled operators, as well as advanced laboratory conditions.[15,16] Therefore, rapid, inexpensive and portable viral load monitoring tools are urgently needed to monitor AIDS patients to expand access to ART in developing countries.

Microfluidic devices have been widely used to develop POC diagnostics due to portability, shortened turnaround time and enhanced sensitivity. However, there are two main challenges, (i) sensitivity, and (ii) subtype coverage, to develop microfluidic-based HIV viral load monitoring tools for POC applications. Although the WHO recommends a viral load of 10 000 copies per millilitre as a clinical cutoff to initiate ART in developing countries,[17] it has also been suggested that a viral load ranging from 1000 to 5000 copies per mL can be used to reduce treatment failure.[18–20] This clinical cutoff range requires microfluidic devices to capture HIV particles at a high efficiency when using small volumes of whole blood. Thus, efficient antibody immobilization is needed to capture HIV particles from whole blood and to meet the requirements of clinical sensitivity. The second challenge to develop HIV viral load devices is based on the global distribution of HIV subtypes, because various non-B HIV

[a]*Demirci Bio-Acoustic-MEMS in Medicine (BAMM) Laboratory, Harvard-MIT Health Sciences and Technology, Department of Medicine, Brigham and Women's Hospital, Harvard Medical School, 65 Landsdowne St., # 267, Cambridge, MA 02139, USA. E-mail: udemirci@rics.bwh.harvard.edu*
[b]*Section of Retroviral Therapeutics, Brigham and Women's Hospital, Harvard Medical School, Boston, MA 02115, USA*
[c]*Harvard-MIT Health Sciences and Technology, Cambridge, MA 02139, USA*
† The authors contributed equally to this work.

subtypes are dominant in resource-constrained settings.[21–23] Although it has been demonstrated that HIV and other virus particles can be efficiently captured by immobilized antibodies in microfluidic systems,[24–26,30,44] the broad applicability of such an approach to capture representative HIV subtypes dominated in developing countries has not been evaluated. The use of polyclonal antibodies that target multiple epitopes of gp120 can provide a niche to capture various HIV subtypes.[27–29]

Here, we present for the first time a microfluidic approach that was used to capture multiple HIV subtypes. We evaluated the optimal antibody immobilization on-chip using Protein G, NeutrAvidin, passive adsorption and covalent binding based approaches. *Via* the Protein G-based antibody immobilization, HIV subtypes of A, B and C were captured at high efficiencies by polyclonal anti-gp120 antibody from culture supernatant and spiked whole blood at viral loads ranging from 1000 to 10 000 copies per mL. These results indicated that various HIV subtypes can be efficiently captured on-chip *via* Protein G-based antibody immobilization, which enables the development of POC viral load devices when combined with on chip detection technologies.

Methods and materials

1. Chemical reagents

Ethanol (200 proof) and glass slides (Gold Seal® Cover glass—24 mm × 40 mm no. 1) were purchased from Fisher Scientific (Fair Lawn, NJ). (3-Mercaptopropyl)trimethoxysilane (3-MPS), dimethyl sulfoxide (DMSO) and lyophilized bovine serum albumin (BSA) were obtained from Aldrich Chemical Co. (Milwaukee, WI). *N*-γ-Maleimidobutyryloxy succinimide ester (GMBS), recombinant Protein G, and NeutrAvidin™ protein were obtained from Pierce Biotechnology (Rockford, IL). Phosphate buffered saline (PBS, pH = 7.4, 1×) was purchased from Invitrogen Co. (Carlsbad, CA). Nonbiotinylated and biotinylated goat anti-HIV gp120 antibody was obtained from Abcam Inc. (Cambridge, MA). Anti-HIV1 gp120 (FITC) polyclonal goat antibody was purchased from Thermo Fisher Scientific (Rockford, IL). Quantum dots (QDs, Qdot® 655 streptavidin conjugate) were purchased from Invitrogen Co. (Carlsbad, CA).

2. Microfluidic device fabrication

Microfluidic channels were fabricated without utilizing photolithographic methods or a clean room.[4,30,31,45,46] Briefly, an inlet and outlet (0.65 mm in diameter, 26 mm apart) were formed in poly(methyl methacrylate) (PMMA) chips (24 × 40 × 1.5 mm) using a VersaLASER cutting machine (Universal Laser Systems Inc., Scottsdale, AZ). Using the same technique, double-sided adhesive (DSA) film (iTapestore, Scotch Plains, NJ) was cut to suit the size of the PMMA chip and contained a carved 28 × 4 mm channel. The prepared DSA was then attached to the PMMA chip to contain an inlet and outlet within the DSA film. A glass slide was treated with oxygen plasma (100 mW, 1% oxygen) for 60 seconds in a PX-250 chamber (March instruments, Concord, MA) and then assembled right away with the PMMA–DSA construct to form a microfluidic channel.

3. Antibody immobilization methods

Four antibody immobilization methods, *i.e.*, passive adsorption, GMBS-based covalent binding, NeutrAvidin–biotin based antibody immobilization, and Protein G-based antibody immobilization, were studied (Fig. 1). For the passive adsorption method, 10 μL of antibody solution was directly incubated in microchannels at room temperature for an hour. The channels were then washed three times with PBS prior to use. For covalent binding, 10 μL of silanization solution (3-MPS) was incubated in the channels for 30 minutes. Channels were then washed three times with ethanol, followed by injection of 2 M GMBS solution and incubation for 35 minutes. The GMBS solution was prepared by diluting the stock solution (50 mg of GMBS in 0.5 mL DMSO) in ethanol. Channels were subsequently washed once with ethanol and three times with PBS. Following this step, 10 μL of antibody solution was incubated in the channels, which were washed three times with PBS. For the NeutrAvidin-based method, channels were prepared as previously described.[4,30] Briefly, 10 μL of NeutrAvidin solution (3 mg mL^{-1}) was incubated in the channels, which were functionalized with GMBS as described above for 1 hour at 4 °C. Then, the channels were incubated with 10 μL of antibody solution at 4 °C for an hour and washed three times with PBS.

For the Protein G-based method, channels functionalized with GMBS were first incubated with Protein G solution and then with anti-gp120 antibody solution at 4 °C for one hour. During optimization of the Protein G-based antibody immobilization, varying concentrations of Protein G (0, 0.03, 0.1, 0.3, 1, 3, 10 mg mL^{-1}) were used. For comparison with passive adsorption and covalent binding, 1 mg mL^{-1} FITC-conjugated anti-gp120 antibody was incubated for an hour at 4 °C. To increase the antibody density on the surface, varying concentrations of FITC-conjugated anti-gp120 antibody (0, 0.05, 0.1, 0.2, 0.5, 0.8, and 1 mg mL^{-1}) were injected in non-treated, GMBS-functionalized, and Protein G-coated (3 mg mL^{-1}) channels.

4. Antibody density measurement by fluorescence imaging and analysis

Two types of fluorescent materials were used in this study: FITC-conjugated antibodies and streptavidin-coated QDs. For comparison of passive adsorption, covalent binding and Protein G-based surface chemistry, FITC-conjugated anti-gp120 antibody was used. The green fluorescence signals were detected using a GFP filter (GFP, 489 nm/509 nm) by an inverted fluorescent microscope (10×, Axio Observer D1, Carl Zeiss, Germany). Green fluorescence images were taken with an exposure time of 400 ms. For comparison of NeutrAvidin and Protein G-based surface chemistry, 20 nM of streptavidin-conjugated QDs were used. The red QD signals were imaged using the inverted fluorescent microscope (10×, Axio Observer D1, Carl Zeiss, Germany). QD655 was detected with the Alexa Fluor® 568 filter (578 nm/603 nm) and fluorescence images were taken with an exposure time of 700 ms. Due to the variations in fluorescence intensity observed between experiments, the device operation and imaging were performed on the same day. Five representative fluorescence images (with dimensions of 660 μm by 3.1 mm) from each channel were taken using the microscope and the

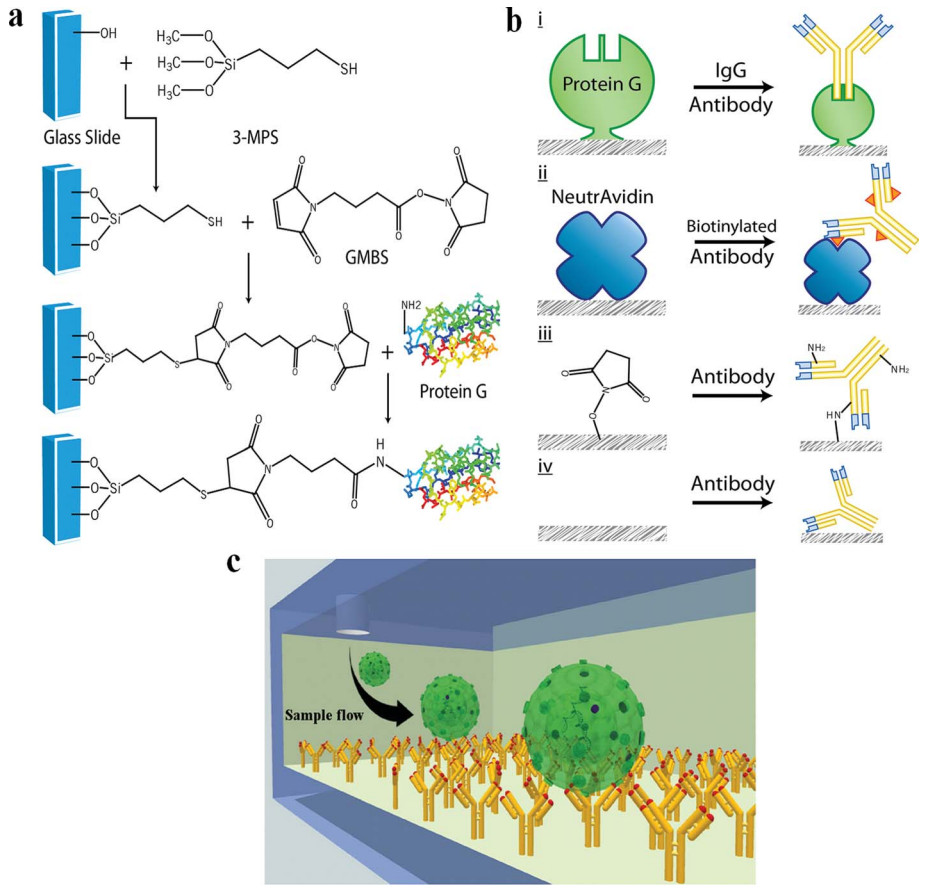

Fig. 1 Surface chemistry of antibody immobilization to capture HIV in a microfluidic device. (a) Protein G-based antibody immobilization. (b) Four methods used for immobilizing antibodies on the glass surface: (i) IgG antibodies bind to Protein G, (ii) biotinylated antibodies bind to NeutrAvidin molecules, (iii) antibodies bind to GMBS, and (iv) antibodies were passively adsorbed on the glass surface. (c) Capture of HIV in channels immobilized with anti-gp120 antibody.

fluorescence intensity of each image was analyzed with the aid of software ImageJ (http://rsbweb.nih.gov/ij/). The average pixel intensity was obtained and reported in arbitrary units (0–255 AU).

5. Nanoscale surface characterization with AFM

The roughness and orientation of the coated antibody for all surface chemistry methods were analyzed using AFM. The glass substrate, which was used to assemble channels, was washed with ultrapure water (Mili-Q®, Millipore Co., Billerica, MA) after surface chemistry. To analyze biological samples by AFM, we used native conditions which do not damage the structure and function of biological components. The glass substrate was then detached from the channel and used for AFM analysis. The glass substrate was then analyzed using the Asylum-1 MFP-3D AFM system (Asylum Research Inc., Santa Barbara, CA). The AC240FS cantilever (Olympus Co., Tokyo, Japan) with 70 kHz resonance frequency and 2 N m^{-1} spring constant was used to probe the thickness and density of coated protein on the surface. The glass substrate was probed at 1 Hz frequency on five random 1 μm × 1 μm spots. Root mean square (RMS) values from each spot were calculated and averaged from 5 AFM images.

6. Quantification of HIV by RT-qPCR

For HIV testing, we captured HIV from two types of HIV samples, *i.e.*, HIV culture supernatant and whole blood spiked with HIV. 10 μL of cultured HIV supernatant (1000, 10 000, and 100 000 copies per mL) or 10 μL of whole blood spiked with HIV (with a final concentration of 1000, 10 000, and 100 000 copies per mL) was flowed into a channel immobilized with anti-gp120 *via* Protein G and the HIV sample was incubated in the channel for 5 minutes at ambient temperature. This virus capture step was repeated 10 times and a total of 100 μL of HIV supernatant or spiked whole blood was flowed through the channel.

The captured virus particles were lysed using guanidine isothiocyanate provided in the QIAamp Viral RNA Mini Kit (Qiagen, Valencia, CA). The lysate was used for HIV RNA extraction according to the manufacturer's instructions. HIV RNA was quantified using reverse transcription-quantitative polymerase chain reaction (RT-qPCR).[32] In the reverse transcription reaction (20 μL), there was 10 μL of 2× core RT buffer, 2 μL of 10 μM of reverse primer (5′-GTCTGAGG GATCTCTCTAGTTACCAG-3′), 0.5 μL of AffinityScript (Applied Biosystems, Carlsbad, CA), and 7.5 μL of HIV RNA. The RT reaction was performed on the GeneAmp PCR System 9700 (Applied Biosystems, Carlsbad, CA) with a program of

25 °C for 5 minutes, 45 °C for 60 minutes and 95 °C for 3 minutes. In qPCR, 50 μL of the master mixture consisted of 1× core PCR buffer, 0.4 μM of forward primer LTR-F (5′-TAAAGCTTGCCTTGAGTGCT-3′) and reverse primer LTR-R2, 0.2 μM of TaqMan probe LTR-P (5′-AGTAGTGT GTGCCCGTCTGTTGTGTG-3′, JOE as the fluorophore and TAMRA as the quencher), 2.5 U of SureStart Taq polymerase, and 10 μL of cDNA template. The amplification reaction was performed on the 7300 Real-Time PCR System (Applied Biosystems, Carlsbad, CA) with a protocol of 25 °C for 5 minutes and 95 °C for 10 minutes, which was followed by 50 cycles of 60 °C for 1 minute and 95 °C for 30 seconds.

Results and discussion

1. Optimization of Protein G-based antibody immobilization

To find the optimal concentration of Protein G for antibody immobilization, varying concentrations of Protein G were incubated in functionalized channels prior to fluorescent antibody (FITC conjugated anti-gp120 antibody) incubation. As shown in Fig. 2a, the average channel fluorescence intensity increased with Protein G concentrations (0–10 mg mL^{-1}), indicating that more antibodies were immobilized on the surface at higher concentrations of Protein G. We observed that the increase of antibody density did not linearly correlate with the increase of Protein G concentration (Fig. 2a). Once the Protein G concentration was more than 3 mg mL^{-1}, the fluorescence intensity only increased by 16.6% compared to the fluorescence intensity at 3 mg mL^{-1} of Protein G. In comparison, the fluorescence intensity increased by 83.3% when the Protein G concentration increased from 0 to 3 mg mL^{-1}. Thus, 3 mg mL^{-1} of Protein G was used to immobilize antibodies on the microchannel surface for the rest of the experiments.

Initially, passive adsorption and GMBS-based covalent binding were compared to the developed Protein G-based surface chemistry in terms of the antibody binding capacity using FITC-conjugated anti-gp120 antibody (Fig. 2b). Varying concentrations (0.05, 0.1, 0.2, 0.4, 0.8, and 1 mg mL^{-1}) of FITC-conjugated anti-gp120 antibody were incubated in non-treated channels (passive adsorption), GMBS-functionalized channels, and Protein G-coated channels. Average fluorescence intensity values in channels with different coatings were presented as a function of antibody concentration (Fig. 2b). We observed that increasing the concentration of antibody immobilized in the channels dramatically enhanced the fluorescence intensity for Protein G-coated (3 mg mL^{-1}) channels, whereas there was only a slight increase in GMBS-coated or non-treated channels (Fig. 2b). GMBS coated channels showed comparable fluorescence intensities in microchannels without surface coating (passively adsorbing channels). As the antibody concentration exceeded 0.05 mg mL^{-1}, the fluorescence signal gradually saturated GMBS coated and non-treated channels due to the limited capability to immobilize FITC-antibody on the surface. At the Protein G concentration of 3 mg mL^{-1}, the fluorescence intensity of Protein G channel was twelve-fold greater than that of GMBS-coated and passive adsorption channels, indicating that the capture efficiency can be significantly increased *via* Protein G-based surface chemistry. In addition, for Protein G based channels, the antibody concentration did not increase the fluorescence intensity once it was above 0.4 mg mL^{-1}. 1 mg mL^{-1} of antibody concentration resulted in saturated fluorescence signals (Fig. 2b).

2. Comparison of Protein G and NeutrAvidin based antibody immobilization using QDs

NeutrAvidin was used to immobilize biotinylated antibody in immunoassays.[30,33,34] To compare the antibody binding capacity of NeutrAvidin and Protein G-based surface chemistry, QDs were used to facilitate fluorescence imaging and the fluorescence intensities in microchannels were recorded. We first analyzed non-specific binding of QDs in microchannels and investigated the capability of BSA to reduce non-specific binding of QDs

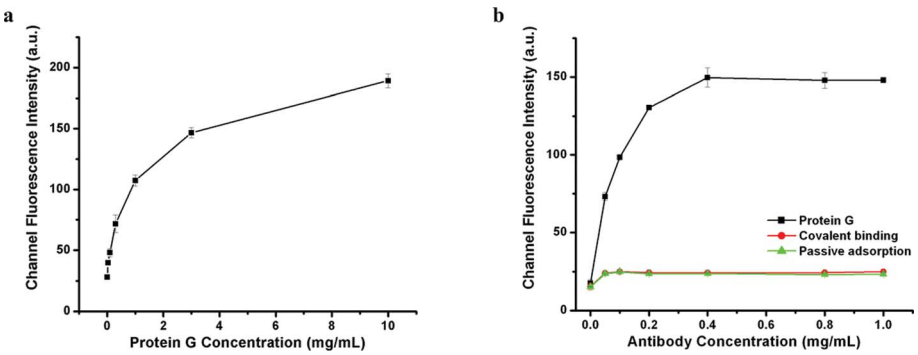

Fig. 2 Optimization of Protein G-based antibody immobilization. FITC-conjugated anti-gp120 antibody was used to facilitate the fluorescence staining in microchannels. (a) Protein G-based antibody immobilization was optimized by varying Protein G concentrations in the microchannels before antibody incubation. The GMBS functionalized channels were first incubated with Protein G at concentrations of 0, 0.03, 0.1, 0.3, 1, 3, 10 mg mL^{-1} and then incubated with 1 mg mL^{-1} solution of FITC-conjugated anti-gp120 antibody at 4 °C for 1 hour. Data are presented as average ± SD ($n = 18$). (b) Comparison of Protein G-based antibody immobilization with passive adsorption and GMBS based covalent binding. In the passive adsorption method, fluorescent antibody was directly injected into channels. In GMBS based covalent binding, microchannels were functionalized with GMBS and then injected with the fluorescent antibody. In the Protein G-based antibody immobilization, functionalized channels were coated with Protein G (3 mg mL^{-1}) and then the fluorescent antibody. In these three methods, varying concentrations of FITC-conjugated anti-gp120 antibody (0, 0.05, 0.1, 0.2, 0.4, 0.8, and 1 mg mL^{-1}) were injected. Data are presented as average ± SD ($n = 18$).

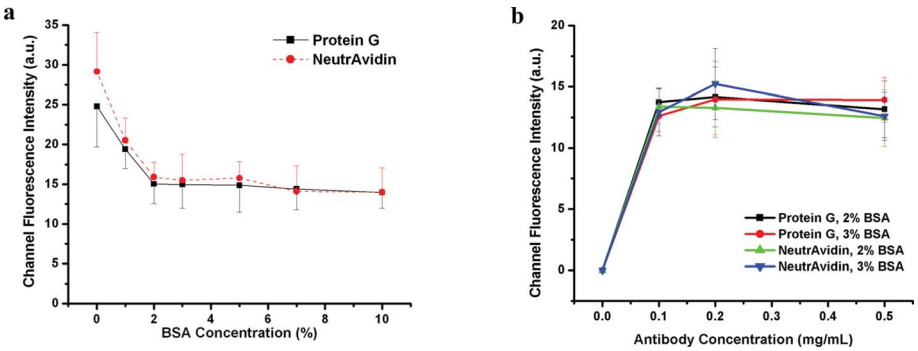

Fig. 3 Comparison of NeutrAvidin and Protein G-based antibody immobilization. Streptavidin conjugated QDs 655 was used to facilitate the fluorescence staining to compare these two methods. Because of non-specific binding of streptavidin conjugated QDs 655 on the channel surface, the channel surface was blocked with varying concentrations of BSA before fluorescence staining. (a) Removal of non-specific binding by varying BSA concentrations in microchannels. Following the surface functionalization with GMBS, channels were incubated with either 3 mg mL^{-1} NeutrAvidin or 3 mg mL^{-1} Protein G for one hour at 4 °C. Biotinylated anti-gp120 antibody (1 mg mL^{-1}) was then incubated in all channels at 4 °C for one hour. BSA solutions with varying concentrations (0, 1, 2, 3, 5, 7, and 10%) were incubated in channels at 4 °C for 1 hour. For fluorescence imaging, both channels were incubated with streptavidin conjugated QDs 655 at ambient temperature for 10 minutes. Data are presented as average ± SD ($n = 15$). (b) Comparison of NeutrAvidin and Protein G-based antibody immobilization by varying antibody concentrations in the presence of 2% and 3% of BSA. The same protocol was used as described above except that 2% and 3% BSA was used to remove the non-specific binding of QDs 655. Data are presented as average ± SD ($n = 15$).

(Fig. 3a). The fluorescence intensity in both channels was approximately 25 AU in the absence of BSA blocking due to non-specific binding of QDs. When BSA (1%) was applied after the antibody immobilization, the fluorescence intensity significantly reduced, indicating that BSA blocked the binding sites on the substrate surface in channels coated with Protein G (red line) and NeutrAvidin (black line). Although NeutrAvidin-coated channels demonstrated a slightly higher intensity at lower BSA concentrations, the fluorescence intensity leveled off at 15 AU at 2% BSA, which was in accordance with the concentrations of BSA (1–3%) used in immunoassays. Thus, we used 2% and 3% of BSA to reduce non-specific binding of QDs in the following evaluation to compare NeutrAvidin and Protein G-based antibody immobilization (Fig. 3b). The results showed that both

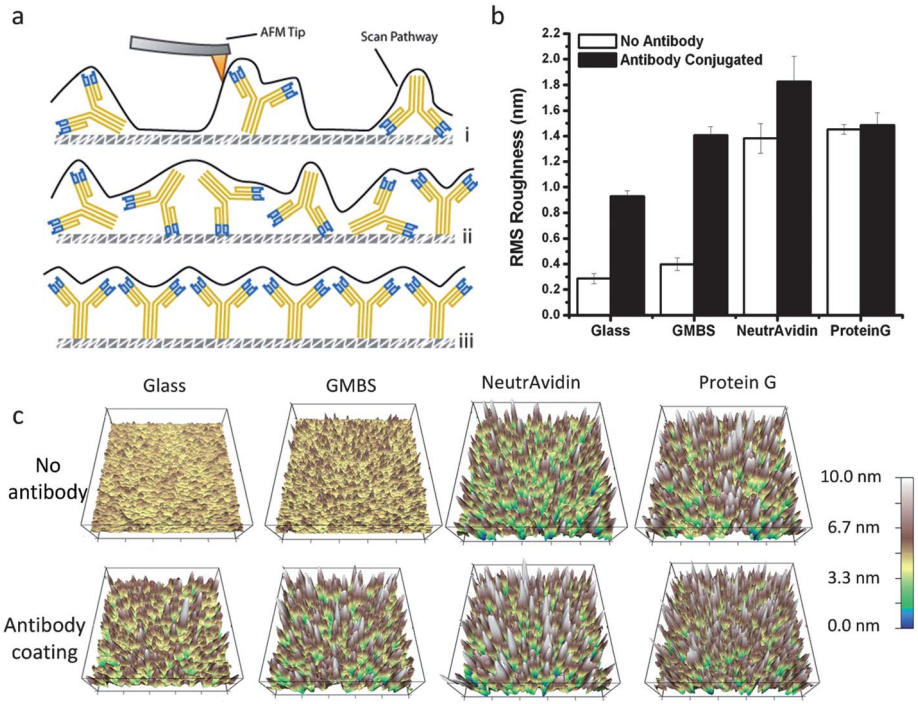

Fig. 4 AFM analysis of antibody immobilization. (a) Schematic of antibody immobilization measured by AFM: (i) low antibody density, (ii) high density randomly oriented antibodies, and (iii) high density uniformly oriented antibodies. (b) Surface roughness of four different surface chemistry methods measured by AFM. Five random 1 μm × 1 μm locations on each surface was probed, and RMS values were calculated. Data are presented as average ± SD ($n = 5$). (c) Typical morphology of the probed surfaces immobilized with four different surface chemistry methods.

methods enhanced the fluorescence to 15 AU compared to the control. The results indicated that both methods immobilized comparable amounts of antibody on the surface.

The Protein G-based antibody immobilization provides an alternative to conventional NeutrAvidin based surface chemistry. In addition, both Protein G and NeutrAvidin based surface chemistry can be used simultaneously for capture and detection. For instance, a virus can be captured by Protein G-based surface chemistry using anti-gp120 antibody. Then, the same gp120 receptor on the captured virus can be used for labeling and detection using streptavidin coated QDs. Thus, the separation of capture and detection chemistries can potentially lower the non-specific binding, and enhance detection outcomes. In the next section, we further characterized the surface features of these four methods (Protein G and NeutrAvidin based surface chemistries) using AFM analysis.

3. Nanoscale surface characterization with AFM

Theoretically, the method that has a more favorable antibody orientation would have a higher capture efficiency at a similar antibody density immobilized on a surface. To evaluate antibody orientation after immobilization, we used AFM to analyze the surface roughness for all evaluated surface chemistry methods. Surfaces with uniform distribution of antibodies are expected to result in lower changes in surface roughness (Fig. 4a). As shown in Fig. 4b and c, a significant difference in surface roughness was observed before and after antibodies were immobilized on glass and glass treated with GMBS surfaces. Lower differences in surface roughness were observed before and after antibodies were immobilized by Protein G-based surface chemistry compared to NeutrAvidin-based surface chemistry. The low difference in surface roughness before and after the immobilization step indicates favorable antibody orientation, since the AFM tip cannot detect trenches on the surface to measure roughness (Fig. 4a).[35] Since Protein G immobilizes the IgG antibody at the Fc section, Fab of the immobilized antibody is favorably placed upright to capture biological moieties.[36] In comparison, NeutrAvidin immobilizes the antibody *via* biotin–NeutrAvidin interaction. However, the position of biotin on biotinylated antibodies may vary.[37] This may result in a less uniform antibody orientation as indicated by the roughness changes compared to Protein G-based surface chemistry (Fig. 4b).

4. Capture efficiency assessment by PCR

Via the Protein G-based surface chemistry, we immobilized anti-gp120 antibody to capture HIV particles in a microfluidic device (Fig. 5a) and characterized the capture efficiency by RT-qPCR (Fig. 5b and c). The results showed that HIV particles of subtypes A, B and C were efficiently captured from viral culture

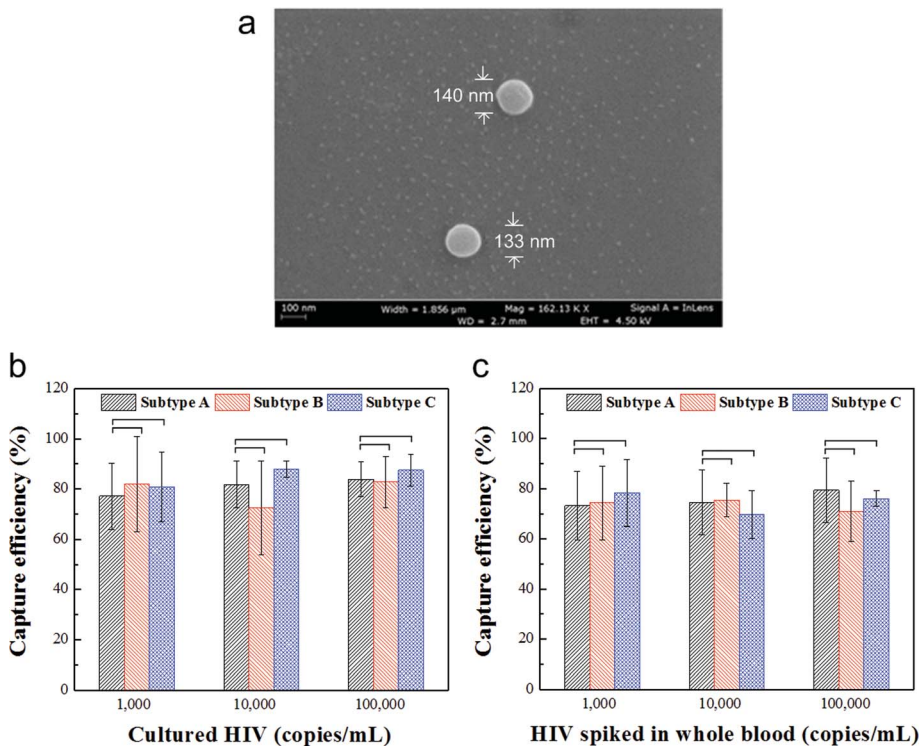

Fig. 5 Application of Protein G-based antibody immobilization to capture HIV particles in microfluidic devices. (a) SEM image of captured HIV particles. After antibody immobilization, the bottom of the microchannel (a glass slide) that contained the captured HIV particles was cut by a glass cutter and then prepared for SEM imaging. SEM image was taken at 2.7 working distance and 4.50 kV accelerating voltage. Capture efficiency of HIV subtypes A, B and C from culture supernatant (b) and whole blood (c) *via* Protein G-based surface chemistry. 100 μL of HIV samples (1000, 10 000 and 100 000 copies per mL) were flowed into microchannels and incubated for 5 minutes at room temperature. The channels were washed with 20 μL of PBS. The captured virus was then removed by adding the lysis buffer and subsequently quantified by RT-qPCR. Data are presented as average ± SD ($n = 4$). No significant difference was observed in the capture efficiency of subtypes A, B and C.

supernatant and spiked whole blood. For culture supernatant samples, the capture efficiency of subtype A was 77.2 ± 13.2, 81.9 ± 9.4 and 83.9 ± 6.9%; the capture efficiency of subtype B was 82.1 ± 18.8, 72.5 ± 18.7, 82.8 ± 10.2% and the capture efficiency of subtype C was 80.9 ± 14.0, 87.8 ± 3.2 and 87.6 ± 6.4% for viral loads of 1000, 10 000, and 100 000 copies per mL, respectively. For whole blood spiked with HIV, the capture efficiency of subtype A was 73.2 ± 13.6, 74.6 ± 12.9 and 79.4 ± 12.9%; the capture efficiency of subtype B was 74.4 ± 14.6, 75.5 ± 6.7, 71.1 ± 12.1% and the capture efficiency of subtype C was 78.3 ± 13.3, 69.7 ± 9.5 and 76.0 ± 3.1% for viral loads of 1000, 10 000, and 100 000 copies per mL, respectively. The high capture efficiency in this study is facilitated by the enhanced density of anti-gp120 antibody with favorable orientation using Protein G-based surface chemistry.

Most importantly, comparable capture efficiency was obtained between subtypes A, B and C. The data indicated that anti-gp120 antibody can be potentially used as a generic capture moiety to capture various HIV subtypes. A number of studies have shown that HIV can quickly modify gp120 epitopes by glycosylation modifications,[40–42] thus evading the neutralization by host anti-gp120 antibodies. Due to the lack of selection pressure exerted by the human immune system, the lab strains can maintain their phenotypes without dramatic modification in the genome or gp120 antigen, thus rendering stable affinity with the polyclonal anti-gp120 antibody that was used. Although HIV subtypes vary in its RNA genome and surface protein to escape the host immune system, studies have shown that V1–V5 loops within the gp120 antigen contain several discontinuous conserved epitopes that can elicit broadly neutralizing antibodies.[28,38] There are conserved epitopes on gp120, *via* which HIV enters $CD4^+$ T lymphocytes *via* gp120–CD4 interaction.[27,29,39] The capture efficiency and subtype coverage can be further improved by using a broadly neutralizing antibody, which has been identified to facilitate vaccine development.[43]

Conclusion

In conclusion, we demonstrated repeatable, efficient and reliable capture of HIV subtypes (*i.e.*, A, B and C) in a microchip through Protein G-based surface chemistry. Protein G-based surface chemistry can efficiently immobilize high densities of antibodies with favorable orientation to capture viruses for biosensing applications such as microchip-based HIV viral load tests at the POC. We compared this method to other antibody immobilization methods including passive adsorption, covalent binding, and NeutrAvidin based surface chemistry. The results showed that the Protein G-based surface chemistry had a twelve-fold increase in immobilized antibody density compared to passive adsorption and covalent binding. Although the NeutrAvidin based antibody immobilization showed comparable antibody density through fluorescence microscopy analysis, Protein G-based surface chemistry poses a better control over the antibody orientation on the surface. This platform technology can be potentially used to measure HIV-1 viral load in resource-constrained settings. Protein G-based surface chemistry when used together with NeutrAvidin based surface chemistry enables the separation of capture and detection chemistries that can potentially reduce the non-specific binding, and enhance detection outcomes. The presented microchip takes an enabling step towards viral load ART monitoring in resource-constrained settings.

Acknowledgements

We would like to acknowledge the W. H. Coulter Foundation Young Investigator Award, RO1 A1081534, R21 AI087107. This work was supported by the Center for Integration of Medicine and Innovative Technology (CIMIT) under U.S. Army Medical Research Acquisition Activity Cooperative Agreements DAMD17-02-2-0006, W81XWH-07-2-0011, and W81XWH-09-2-0001. And this work was made possible by a research grant that was awarded and administered by the U.S. Army Medical Research & Materiel Command (USAMRMC) and the Telemedicine & Advanced Technology Research Center (TATRC), at Fort Detrick, MD.

References

1 UNAIDS, 2010, http://www.unaids.org/globalreport/global_report.htm.
2 X. Cheng, Y. S. Liu, D. Irimia, U. Demirci, L. Yang, L. Zamir, W. R. Rodriguez, M. Toner and R. Bashir, *Lab Chip*, 2007, **7**, 746–755.
3 U. A. Gurkan, S. Moon, H. Geckil, F. Xu, S. Wang, T. J. Lu and U. Demirci, *Biotechnol. J.*, 2011, **6**, 138–149.
4 S. Moon, H. O. Keles, A. Ozcan, A. Khademhosseini, E. Haeggstrom, D. Kuritzkes and U. Demirci, *Biosens. Bioelectron.*, 2009, **24**, 3208–3214.
5 A. Ozcan and U. Demirci, *Lab Chip*, 2008, **8**, 98–106.
6 S. Moon, U. A. Gurkan, J. Blander, W. W. Fawzi, S. Aboud, F. Mugusi, D. R. Kuritzkes and U. Demirci, *PLoS One*, 2011, **6**, e21409.
7 M. A. Alyassin, S. Moon, H. O. Keles, F. Manzur, R. L. Lin, E. Haeggstrom, D. R. Kuritzkes and U. Demirci, *Lab Chip*, 2009, **9**, 3364–3369.
8 J. V. Jokerst, P. N. Floriano, N. Christodoulides, G. W. Simmons and J. T. McDevitt, *Lab Chip*, 2008, **8**, 2079–2090.
9 X. Cheng, D. Irimia, M. Dixon, K. Sekine, U. Demirci, L. Zamir, R. G. Tompkins, W. Rodriguez and M. Toner, *Lab Chip*, 2007, **7**, 170–178.
10 X. Cheng, D. Irimia, M. Dixon, J. C. Ziperstein, U. Demirci, L. Zamir, R. G. Tompkins, M. Toner and W. R. Rodriguez, *JAIDS, J. Acquired Immune Defic. Syndr.*, 2007, **45**, 257–261.
11 D. K. Glencross, G. Janossy, L. M. Coetzee, D. Lawrie, H. M. Aggett, L. E. Scott, I. Sanne, J. A. McIntyre and W. Stevens, *Cytometry, Part B*, 2008, **74**(Suppl 1), S40–S51.
12 J. J. G. van Oosterhout, L. Brown, R. Weigel, J. J. Kumwenda, D. Mzinganjira, N. Saukila, B. Mhango, T. Hartung, S. Phiri and M. C. Hosseinipour, *Trop. Med. Int. Health*, 2009, **14**, 856–861.
13 P. Mee, K. L. Fielding, S. Charalambous, G. J. Churchyard and A. D. Grant, *AIDS*, 2008, **22**, 1971–1977.
14 A. Singh, H. Sunpath, T. N. Green, N. Padayachi, K. Hiramen, Y. Lie, E. D. Anton, R. Murphy, J. D. Reeves, D. R. Kuritzkes and T. Ndung'u, *JAIDS, J. Acquired Immune Defic. Syndr.*, 2011, **58**, 233–240.
15 S. Wang, F. Xu and U. Demirci, *Biotechnol. Adv.*, 2010, **28**, 770–781.
16 W. G. Lee, Y. G. Kim, B. G. Chung, U. Demirci and A. Khademhosseini, *Adv. Drug Delivery Rev.*, 2010, **62**, 449–457.
17 A. Calmy, N. Ford, B. Hirschel, S. J. Reynolds, L. Lynen, E. Goemaere, F. Garcia de la Vega, L. Perrin and W. Rodriguez, *Clin. Infect. Dis.*, 2007, **44**, 128–134.
18 W. S. Stevens, L. E. Scott and S. M. Crowe, *J. Infect. Dis.*, 2010, **201**(Suppl 1), S16–S26.
19 S. Tanriverdi, L. Chen and S. Chen, *J. Infect. Dis.*, 2010, **201**(Suppl 1), S52–S58.
20 M. Usdin, M. Guillerm and A. Calmy, *J. Infect. Dis.*, 2010, **201**(Suppl 1), S73–S77.
21 J. Hemelaar, E. Gouws, P. D. Ghys and S. Osmanov, *AIDS*, 2006, **20**, W13–W23.

22 J. Hemelaar, E. Gouws, P. D. Ghys, S. Osmanov and W.-U.N.H.I. C, *AIDS*, 2011, **25**, 679–689.
23 B. S. Taylor, M. E. Sobieszczyk, F. E. McCutchan and S. M. Hammer, *N. Engl. J. Med.*, 2008, **358**, 1590–1602.
24 R. Dhumpa, M. Bu, K. J. Handberg, A. Wolff and D. D. Bang, *J. Virol. Methods*, 2010, **169**, 228–231.
25 B. C. Kim, M. K. Ju, A. Dan-Chin-Yu and P. Sommer, *Anal. Chem.*, 2009, **81**, 2388–2393.
26 Y. F. Lee, K. Y. Lien, H. Y. Lei and G. B. Lee, *Biosens. Bioelectron.*, 2009, **25**, 745–752.
27 Y. Li, S. A. Migueles, B. Welcher, K. Svehla, A. Phogat, M. K. Louder, X. Wu, G. M. Shaw, M. Connors, R. T. Wyatt and J. R. Mascola, *Nat. Med.*, 2007, **13**, 1032–1034.
28 R. Wyatt, P. D. Kwong, E. Desjardins, R. W. Sweet, J. Robinson, W. A. Hendrickson and J. G. Sodroski, *Nature*, 1998, **393**, 705–711.
29 T. Zhou, L. Xu, B. Dey, A. J. Hessell, D. Van Ryk, S. H. Xiang, X. Yang, M. Y. Zhang, M. B. Zwick, J. Arthos, D. R. Burton, D. S. Dimitrov, J. Sodroski, R. Wyatt, G. J. Nabel and P. D. Kwong, *Nature*, 2007, **445**, 732–737.
30 Y. G. Kim, S. Moon, D. R. Kuritzkes and U. Demirci, *Biosens. Bioelectron.*, 2009, **25**, 253–258.
31 S. Wang, X. Zhao, I. Khimji, R. Akbas, W. Qiu, D. Edwards, D. W. Cramer, B. Ye and U. Demirci, *Lab Chip*, 2011, **11**, 3411–3418.
32 D. Candotti, J. Temple, S. Owusu-Ofori and J. P. Allain, *J. Virol. Methods*, 2004, **118**, 39–47.
33 N. Dinauer, S. Balthasar, C. Weber, J. Kreuter, K. Langer and H. von Briesen, *Biomaterials*, 2005, **26**, 5898–5906.
34 B. M. Lingerfelt, H. Mattoussi, E. R. Goldman, J. M. Mauro and G. P. Anderson, *Anal. Chem.*, 2003, **75**, 4043–4049.
35 X. Wang, Y. Wang, H. Xu, H. Shan and J. R. Lu, *J. Colloid Interface Sci.*, 2008, **323**, 18–25.
36 K. Kato, L. Y. Lian, I. L. Barsukov, J. P. Derrick, H. Kim, R. Tanaka, A. Yoshino, M. Shiraishi, I. Shimada and Y. Arata, *et al.*, *Structure*, 1995, **3**, 79–85.
37 I.-H. Cho, E.-H. Paek, H. Lee, J. Y. Kang, T. S. Kim and S.-H. Paek, *Anal. Biochem.*, 2007, **365**, 14–23.
38 J. Pietzsch, J. F. Scheid, H. Mouquet, F. Klein, M. S. Seaman, M. Jankovic, D. Corti, A. Lanzavecchia and M. C. Nussenzweig, *J. Exp. Med.*, 2010, **207**, 1995–2002.
39 X. Wu, Z. Y. Yang, Y. Li, C. M. Hogerkorp, W. R. Schief, M. S. Seaman, T. Zhou, S. D. Schmidt, L. Wu, L. Xu, N. S. Longo, K. McKee, S. O'Dell, M. K. Louder, D. L. Wycuff, Y. Feng, M. Nason, N. Doria-Rose, M. Connors, P. D. Kwong, M. Roederer, R. T. Wyatt, G. J. Nabel and J. R. Mascola, *Science*, 2010, **329**, 856–861.
40 B. Chackerian, L. M. Rudensey and J. Overbaugh, *J. Virol.*, 1997, **71**, 7719–7727.
41 Y. Li, B. Cleveland, I. Klots, B. Travis, B. A. Richardson, D. Anderson, D. Montefiori, P. Polacino and S. L. Hu, *J. Virol.*, 2008, **82**, 638–651.
42 M. Sagar, X. L. Wu, S. Lee and J. Overbaugh, *J. Virol.*, 2006, **80**, 9586–9598.
43 L. M. Walker, S. K. Phogat, P. Y. Chan-Hui, D. Wagner, P. Phung, J. L. Goss, T. Wrin, M. D. Simek, S. Fling, J. L. Mitcham, J. K. Lehrman, F. H. Priddy, O. A. Olsen, S. M. Frey, P. W. Hammond, S. Kaminsky, T. Zamb, M. Moyle, W. C. Koff, P. Poignard and D. R. Burton, *Science*, 2009, **326**, 285–289.
44 S. Q. Wang, A. Ip, F. Xu, F. F. Giguel, S. Moon, A. Akay, D. R. Kuritzkes and U. Demirci, in *Sensors, and Command, Control, Communications, and Intelligence*, ed. E. M. Carapezza, Spie-Int Soc Optical Engineering, Bellingham, 2010, vol. 7666, DOI: 10.1117/12.853132.
45 U. A. Gurkan, T. Anand, H. Tas, D. Elkan, A. Akay, H. O. Keles and U. Demirci, *Lab Chip*, 2011, **11**, 3979–3989.
46 S. Wang, F. Inci, T. Chaunzwa, A. Ramanujam, A. Vasudevan, S. Subramanian, A. Ip, B. Sridharan, G. GA and U. Demirci, *Int J Nanomedicine*, 2012, DOI: 10.2147/IJN.S29629.